Effective Brain Segmentation Method based on MR Physics Image Processing

Eun-Young Jung[1], Sung-Jong Eun[2] and Dong Kyun Park[*]

[1,]u-Healthcare Center, Gachon University Gil Medical Center, Incheon, Korea*
[2]Department of Computer Science Gachon University, Seongnam, Gyunggi-Do, Korea
eyjung@gilhospital.com[1], asclephios@hotmail.com[2], Pdk66@gilhospital.com[*]

Abstract

Object recognition is usually processed based on region segmentation algorithm. Region segmentation in the IT field is carried out by computerized processing of various input information such as brightness, shape, and pattern analysis. If the information mentioned does not make sense, however, many limitations could occur with region segmentation during computer processing. Therefore, this paper suggests effective region segmentation method based on Susceptibility Weighted Imaging (SWI) within the magnetic resonance (MR) theory. When we do pre-processing, proposed method was composed of SWI process. And then we do the Gray-white matter segmentation by Active Contour Model(ACM) in post-processing. In this study, the experiment had been conducted using images including the brain region and by getting up contrast enhancement image of SWI for segmentation to extract region (white matter) segmentation even when the border line was not clear. As a result, an average area difference of 8.2%, which was higher than the accuracy of conventional region segmentation algorithm, was obtained.

Keywords: *Susceptibility Weighted Imaging (SWI), Brain Segmentation, MR theory, Active Contour Model, Curve Fitting*

1. Introduction

Object recognition is a very important part of image processing. It can begin with area segmentation and image segmentation, which is crucial for image interpretation and is an indispensable stage of image processing. Various image segmentation methods have different characteristics and perform differently according to the input image characteristics; but despite these differences, their image segmentation problems have the same causes. According to the distribution of neighboring pixel values, non-segmentation or excessive segmentation occurs. These problems are common chronic problems with various image segmentation methods, and many studies have been conducted to resolve them.

Generally, image segmentation algorithms include the threshold value technique, the edge detection technique, region growing, and the technique of using texture characteristic values [1-4]. The threshold value method involves creating histograms for the given image, determining the critical value, and partitioning the image into the object and the background. Edge detection refers to the process of looking for gray-level discontinuous pixels in an image. Region growing [5] was designed to measure similarities between pixels to be able to expand and segment an area. In addition, the statistical method and the structural method use texture characteristic values that quantify discontinuous changes in pixel values in an image [6]. In addition to these general methods, methods of segmenting an area manually have been extensively studied, and multi-area segmentation methods are being applied [7]. Of these

(*) corresponding author

methods, the Graph Cut [8] method and the GrabCut [9] method of looking for borders to minimize energy have been proposed as methods of minimizing the involvement of users, but they have the disadvantage of requiring the setting of the initial area. Also, the Region Adaptive Algorithm method of extracting features by area using appropriate methods has been proposed, but it has the weakness of yielding inaccurate results in ambiguous borders. To resolve these shortcomings, the curve fitting method based on regional minimum values is being used. In addition, ACM or the snake method [10] was proposed to converge to the point where the energy value is minimum, to detect the optimal contour line. This snake method requires significant user information involvement, however, and has the problem of the misconception of the energy value in a shady area as a different area. To resolve these problems, diverse snake methods have been proposed [11-12].

Representative image segmentation algorithm stems from the difference in pixel information. The difference in pixel, which is input information, is determined by the difference in brightness or shape/pattern, which is connecting information. However, if the difference cannot be identified from the input information, the accuracy of region segmentation dramatically decreases. This paper suggests an effective segmentation method using magnetic resonance (MR) theory to resolve this problem. Magnetic resonance imaging (MRI) is an examination method that produces images using nuclear magnetic resonance (NMR). Resonance means an amplification reaction to the stimulations having with the same frequencies. NMR method measures the signals that come out from a nucleus when it is stimulated by its own characteristic frequency. Human bodies become feeble magnets in a magnetic field. Because the degree of magnetization differs according to the tissues of a human body, an MRI image can be obtained by measuring and graphing the difference through computer processing [13].

There are three types of MRI images: proton density image, T1 image, and T2 image [14-15]. This paper worked towards improving the quality of an image including the brain region, and tried to isolate the brain region (white matter) from the image using texture analysis method by setting up several region of the brain image. This method does not use the conventional pixel information for input information, but instead uses on Susceptibility Weighted Imaging (SWI) [16].

SWI is a new means to enhance contrast in MR imaging [17-20]. Until recently, with the exception of phase being used for large-vessel flow quantification or for use in inversion recovery sequences, most diagnostic MR imaging relied only on the reading of magnitude information. The phase information was ignored and usually discarded before even reaching the viewing console. Phase images, however, contain a wealth of information about local susceptibility changes between tissues [21-23], which can be useful in measuring iron content and other substances that change the local field. The effects of other background magnetic fields presented a major problem by obscuring the useful phase information. Hence, for nearly 20 years, phase information in flow-compensated sequences went essentially unused as a means to measure susceptibility in clinical MR imaging.

In this paper, we try to enhance the accuracy of object segmentation by using SWI process and improved Snake model in ACM. Generally, segmentation methods require post-processing to improve their accuracy. If the first detection work can minimize errors, however, low-cost post-processing alone can yield effective results. Thus, the post-processing method is improved to focus on the initial snake point allotment, convergence of contour lines, and correction work, and to minimize the post-processing costs of area segmentation algorithms.

2. Proposed Method

In applying the object recognition algorithm, input image characteristics are important. Considering the recognition algorithm's input parameter value, it is assumed that the input image's pre-processing result is the same. Recognizing the brain region (white matter) in an MR image provides important information for deciding on therapy or operation method, as well as identifies diseases in the brain. This paper tries to enhance the accuracy of recognition by using SWI information and improved Snake model. The proposed method works as follows: First, the SWI process in T2 image is calculated; second, the calculated each brain regions by the improved snake model. Figure 1 shows the general algorithm flowchart. Detailed and step-by-step explanation will be given thereafter.

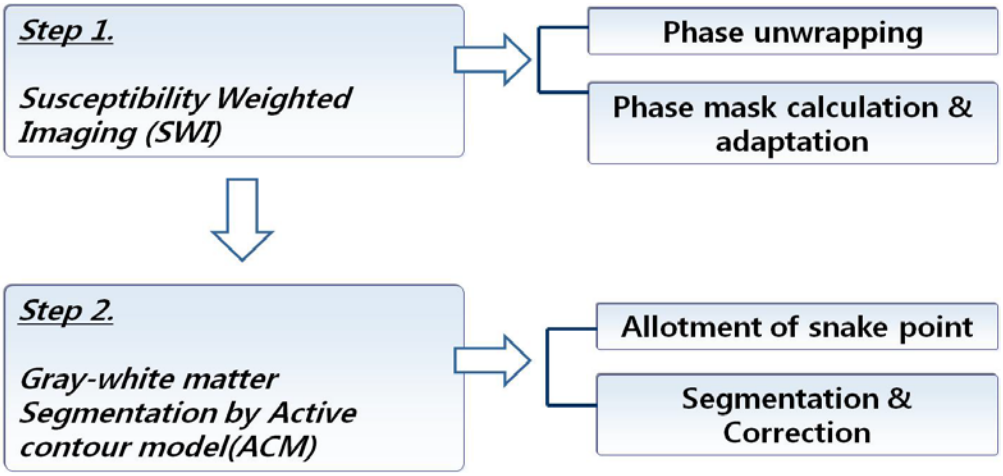

Figure 1. Overview of the Proposed Method

2.1. Susceptibility Weighted Imaging (SWI)

SWI is a new means to enhance contrast in MR imaging. A number of important tissues have unique magnetic susceptibility differences relative to background or surrounding tissues. One such example is partially deoxygenated venous blood [23-25]. Other examples include clot (paramagnetic), calcium (diamagnetic), and iron-laden tissue [26], and air/tissue interfaces. These bulk magnetic susceptibilities are indistinguishable from chemical shift effects.

The most common example of the latter in magnetic resonance imaging (MRI) is the chemical shift difference between water and fat. Usually chemical shift effects are ignored, but in the case of water and fat separation [27-28] the 3.35-ppm difference is used to separate water and fat. On the other hand, if information regarding several species occupying the same voxel is desired, one usually obtains the spectral information by collecting a time series of data and Fourier transforming the data. This is referred to as chemical shift imaging. Since we focus on the role of susceptibility, and use the original phase image both by itself and as a means of altering the contrast in the magnitude images, we refer to this method as SWI [16]. Although SWI has been used as an MR venographic method for several years [29], it has more recently been applied to studies of arterial venous malformations [30], occult venous disease [31], multiple sclerosis [32], trauma [33], tumors [34], and functional brain imaging [35].

Our goal in this part was to use phase to enhance contrast between tissues with different susceptibilities. All the processing steps involved in the creation of susceptibility weighted magnitude images are schematically summarized in Figure 2.

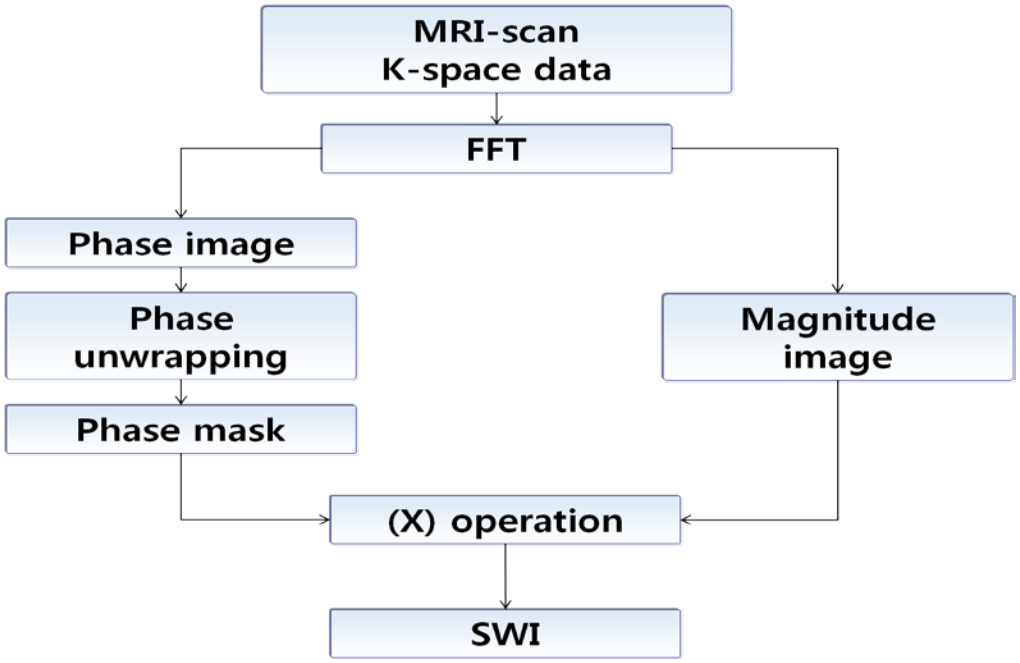

Figure 2. Whole Overview of the SWI Process

2.1.1. Phase Unwrapping

Phase unwrapping is a well-studied but long-standing problem outside the field of MRI. Although many different methods of phase unwrapping have been developed, no general solution is available, particularly in the context of MRI. Mathematically speaking, phase unwrapping can be stated simply as recovering the true phase ϕ from its principal or wrapped value $\phi\wedge$:

$$\phi = \phi\wedge + k \cdot 2\pi \quad (1)$$

where k is an integer and, as explained above, $\phi\wedge$ is limited to a range between - π and π is determined from ϕ through a wrapping operator as follows :

$$\phi\wedge = W[\phi] \quad (2)$$

Phase unwrapping is not meaningful for an isolated image pixel because any multiples of 2 can be added to its principal value. Thus, phase unwrapping is in general only considered for an ensemble of pixels for which the true underlying phase is assumed to be spatially continuous or smooth. We assume that the phase data is spatially smooth and use a Grid-fit method. We propose a more robust and simple phase unwrapping method. The key to our method is to begin the iteration at each grid with least-square fitting by using MiP (Median intensity Projection) process at each axis pixels. Our scheme as the Grid-fit method described in Figure 3. The steps on the proposed Grid-fit method are:

1. Compute phase image in MR T2 scan raw data.
2. Divide by KxK Grid-regions, that Grid-region size can changeable depend on phase image resolution. Sample Grid-region size K is 6 according to Fig. 3.
3. Compute MiP value at each axis pixels.
4. Adjust the Least-square fitting by using MiP values.
5. Fill median value in each pixel by fitted values at local grid.
6. After fit the local grid, adjust the gaussian filtering at entire Grid-region to enhance the global inhomogeneity.

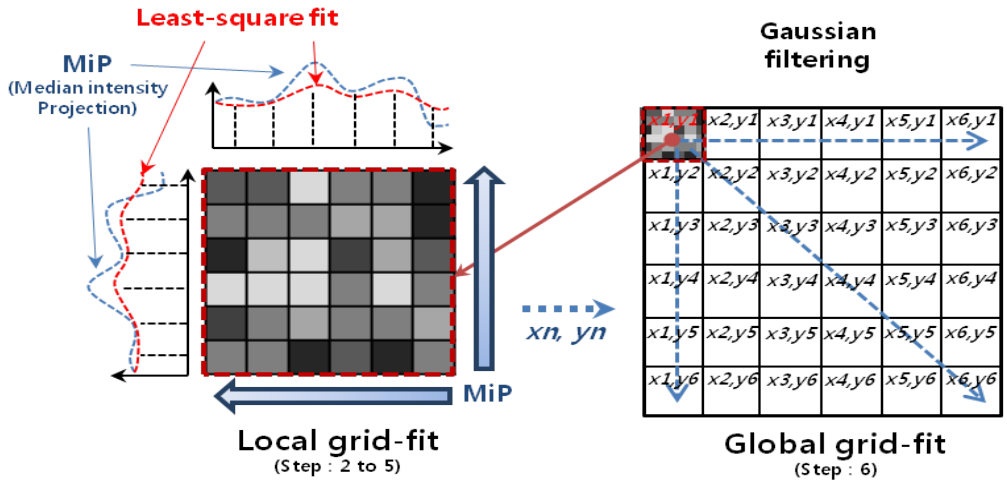

Figure 3. Concept of Grid-fit Phase Unwrapping

Figure 4 shows the results of the unwrapped phase image data by Grid-fit method.

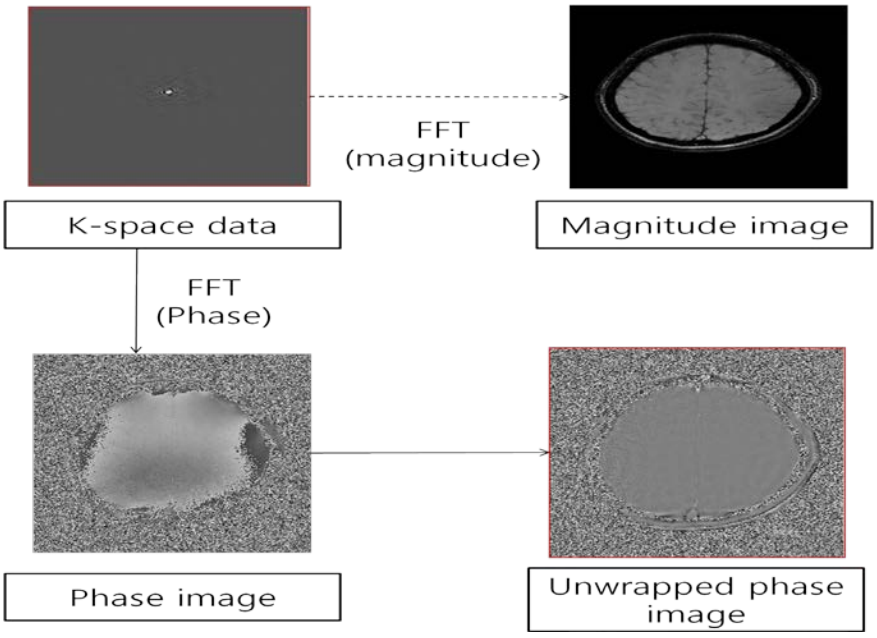

Figure 4. Unwrapped Phase Image Result of Grid-fit Method

2.1.2. Phase Mask Calculation and Adaptation

This unwrapped phase image is used to create a phase mask that is used to multiply the original magnitude image to create novel contrasts in the magnitude image. The phase mask is designed to suppress those pixels that have certain phases. It is usually applied in the following manner: If the minimum phase of interest is, for example, $-\pi$, then the phase mask is designed to be $f(x)(\varphi(x)+\pi)/\pi$ for phases < 0, and to be unity otherwise, where $\varphi(x)$ is the phase at location x. That is, those pixels with a phase of $-\pi$ will be completely suppressed and those with a value between $-\pi$ and zero phase will be only partly suppressed. This phase mask ($f(x)$) then takes on values that lie between zero and unity. We will refer to it as the negative phase mask. It can be applied any number of times (integer m) to the original magnitude image ($\rho(x)$) to create a new image $fm(x)\rho(x)$ with different contrasts[36-37]. Another mask might be defined to highlight positive phase differences by equation 3.

$$\rho(x)_{new} = g^{m}(x)\rho(x) \tag{3}$$

If the maximum phase of interest is, for example, π, then the phase mask is designed to be $g(x) = (\pi-\varphi(x)) / \pi$ for phase > 0, and unity otherwise. We will refer to this as the positive phase mask. And we decide the phase mask multiplication value by some experiments. So we can get the meaningful contrast enhancement image by SWI process.

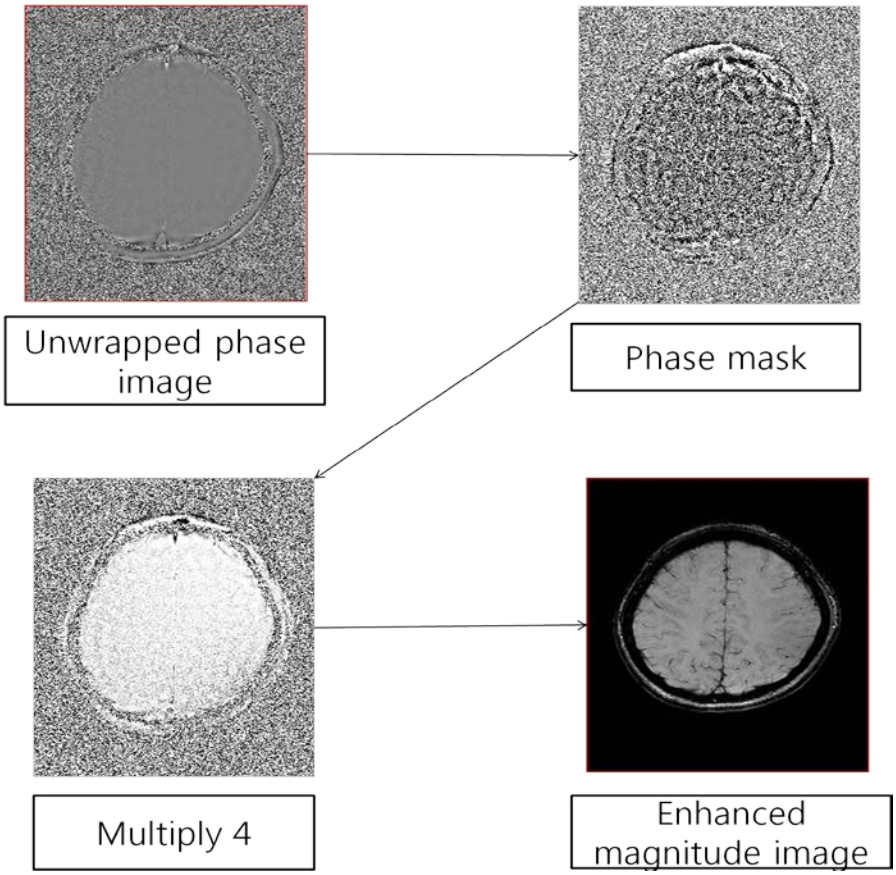

Figure 5. The Result of the SWI Process

2.2. Gray-white Matter Segmentation by ACM

In this phase, the contrast quality of above enhancement result, which have previously been calculated. The candidate boundary line should be using as segmentation boundary in the next step, which uses improved Snake method. Detecting boundary line consists of two tasks. First is limiting the scope of detection. This requires establishing a candidate area to detect boundary line, within which the actual brain region should be detected. Second is identifying the pixels that are considered meaningful as feature points. These feature points are calculated as subtract between original magnitude image and SWI processed magnitude image. And in order to allot the Snake points on boundary line, we use a Mean-shift clustering [38]. Then we used improved Snake method by using this allotted Snake points.

2.2.2. Allotment of Snake Points

These feature points are calculated as subtract between original magnitude image and SWI processed magnitude image. And in order to allot the Snake points on boundary line, we use a Mean-shift clustering. Mean-shift is a procedure for locating the maxima of a density function given discrete data sampled from that function. It is useful for detecting the modes of this density. This is an iterative method, and we start with an initial estimate x. Let a kernel function K(xi, x) be given. This function determines the weight of nearby points for re-estimation of the mean. Typically we use the Gaussian kernel on the distance to the current estimate, the weighted mean of the density in the window determined by K.

$$m(x) = \frac{\sum_{xi \in N(x)} K(xi - x)xi}{\sum_{xi \in N(x)} K(xi - x)} \tag{4}$$

where N(x) is the neighborhood of x, a set of points for which k(x) is not 0. The mean-shift algorithm now sets x : m(x), and repeats the estimation until m(x) converges. And we used improved Snake method by using this allotted Snake points.

2.2.3. White Matter Segmentation by Improved Snake Model

In order to extract the white matter, we use Greedy snake method[39] which performed using the information on the previously calculated Snake points. By concept of Greedy snake method, the energy function $E_{snake}(v_j)$, which moves snake points in a 2D image with the minimum energy value, is expressed as the sum of the internal energy (*i.e.*, the continuity), the curvature energy term, and the external energy term, as shown in the following equation 5.

$$\begin{aligned} E_{snake}(v_j) = \sum_{i=0}^{N-1} [\alpha \cdot E_{continuity}(v_{i,j}) \\ + \beta \cdot E_{curvature}(v_{i,j}) + \gamma \cdot E_{external}(v_{i,j})] \end{aligned} \tag{5}$$

If $v_{i,i} = (x_{i,i}, y_{i,i})$ and i = 0; ...N-1, denoting the total number of snake points, and $x_{i,i}$, $y_{i,i}$ are the x, y coordinates of the i-th snake point of the j-th repetition. The continuous energy minimized the distanced between the snake points obtained at the j+1st repetition to the average distance $\bar{d}_i$ between the snake points at the previous j-th repetition, thereby eventually equalizing the distance between N number of snake points. This snake method considers and converges on only a particular area with a 1x3 mask,

on the basis of the allotted snake points. The particular area is set not to consider unnecessary information when converging contour lines. This is shown in Figure 6.

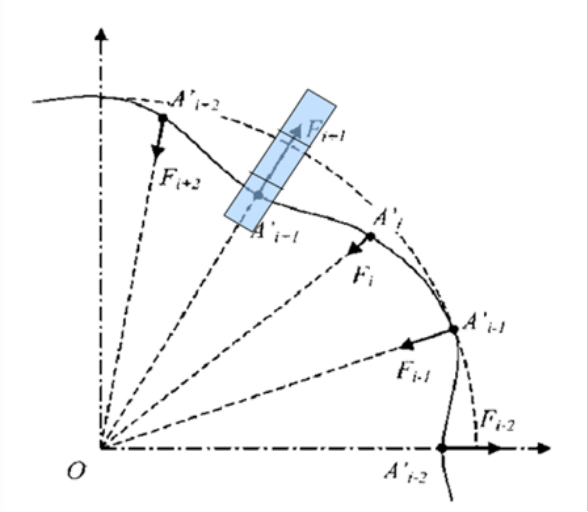

Figure 6. Mask Size (1x3) Decision

Thereafter, the continuous energy is expressed as in Equation 6, and $\overline{d_t}$ is calculated as shown in Equation 7.

$$E_{continuity}(v_{i,j}) = |\overline{d_j} - \| v_{i,j} - v_{i-1,j+1} \||| \tag{6}$$

$$\overline{d_j} = \frac{1}{N}\sum_{i=0}^{N-1} \| v_{i+1,j} - v_{i,j} \| \tag{7}$$

Equation 6 is subject to the condition $v_{0,i} = v_{N,i}$. in which | | is the scalar absolute value and || || is the vector length (Norm). The external energy is generated by various image characteristics such as lines and edges. Generally, energy is used, and a small value is taken in a place with a significant gradient, thereby positioning a snake point on the contour of the relevant object. The external energy is calculated using Equation 8.

$$E_{external}(v_{i,j}) = -|\nabla f(v_{i,j})|^2 \tag{8}$$

In the aforementioned expression, ∇ denotes the gradient, and the energy term's parameters, α, β, γ are weighted, thereby determining the importance of the internal and external energy terms.

The correction method for the snake convergence results begins with the middle point of the initial area set by the user. The contour line correction can be assessed using the following Equation 9.

$$E_{tmp} = \sum_{i=1}^{n} \left| \frac{R_{i-1} + R_{i+1}}{2} - R_i \right| \tag{9}$$

When the allotted snake points are assumed to be in the order of Ri-1, Ri, and Ri+1, the distance between the middle point of the initially set area and each snake point is calculated. If the relevant Ri distance is greater than the average distance of Ri-1 and Ri+1, as in the preceding equation, it is considered problematic. Likewise, the Ri point

is corrected using the linear interpolation of Ri-1 and Ri+1. This interpolation is meant to reduce the post-treatment work, since when conducting contour line convergence work as mentioned in section 2.2.2, three units of snake point convergence work are processed simultaneously. This is shown in Figure 7.

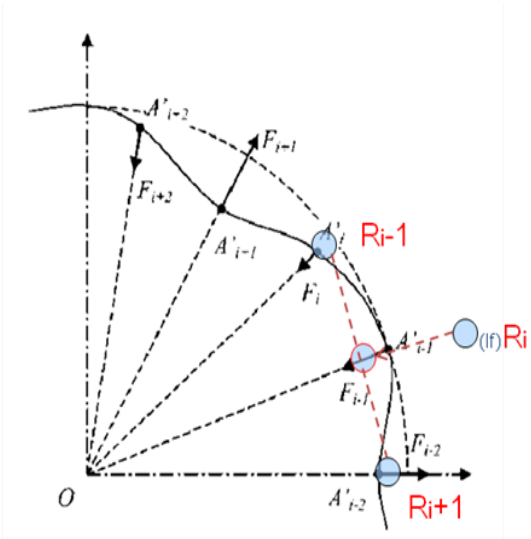

Figure 7. Correction by Linear Interpolation

3. Experiment

To evaluate the proposed method, experiments based on medical MR imaging were performed, and the results were compared with the reference image achieved by a specialist doctor. Thus, the accuracy of the method was evaluated quantitatively. Towards this end, the difference ratio between the reference image and the area from the proposed method was calculated, and can be expressed by the following Equation10.

$$R_{diff} = \frac{|R_{criteria} - R_{proposed}|}{R_{criteria}} \times 100 \quad (10)$$

In Equation 10, R_{diff} denotes the area difference ratio, $R_{criteria}$ denotes the area of the reference image, and $R_{proposed}$ represents the area created by the proposed method. For this experiment, a total of 60 MR images were processed, and the relevant image criteria were evaluated according to the results of the proposed method and of Equation 10, after a specialist doctor established the baseline using Adobe Photoshop CS. In our case, to evaluate the accuracy, we calculate the average area difference by each slice in brain volume data. As a result, an average area difference ratio of 8.2% was determined. Figure 8 shows the some samples of evaluation result in the proposed method.

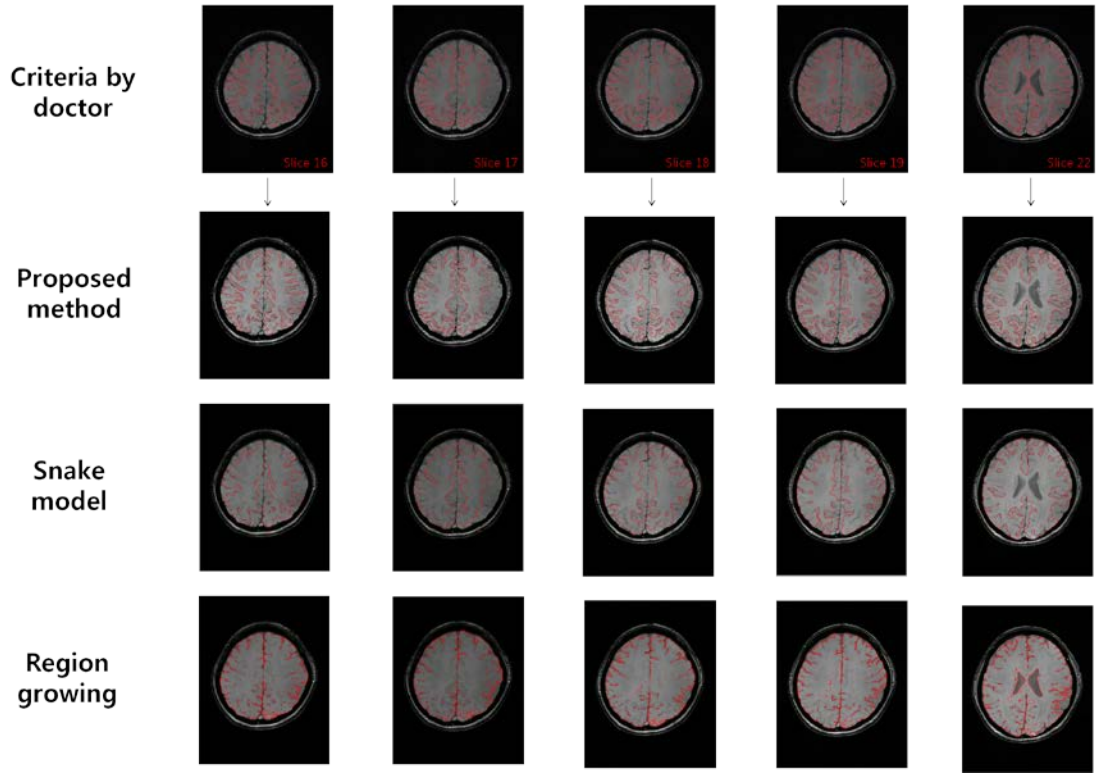

Figure 8. The Comparison Samples of each Final Results

To provide more points for comparison, other techniques were implemented such as the general region growing [5] and Snake method [10] using the slice 60 images in Figure 8 and Table 1 show the sample results of the application of the comparison algorithm.

Actually, proposed method is composed of general segmentation algorithm in addition to MR theory as SWI information. So that's why we choose the comparison method like a region growing and snake model. In case of region growing, seed point is set the manually by criteria boundary. Threshold value was calculated by average intensity. In case of snake model, initial contour set the manually by criteria boundary. According to the results shown in Figure 8 and Table 1, the existing snake method and region growing caused some problems in that the intensity or energy recognized portions with ambiguous shades as different areas.

Table 1. Results of comparison of the proposed method with the other methods

Method	Average area difference ratio
Region Growing	17.5%
Snake	12.2%
Proposed Method	8.2%

3. Conclusion

In this paper, SWI process within the MR theory has been used to resolve the basic limitations in computer processing. It suggested detection of meaningful segmented regions. It also suggested an effective algorithm to detect the brain region using improved Snake model based on SWI image. This method did not stick to fundamental brightness processing, but focused on finding the region that adjust the enhance contrast by SWI processing, considering the functional characteristics of the susceptibility. The results have confirmed that the meaningful region, which have been detected through a corresponding susceptibility, that is, the method in which the brain region detected through SWI were used was more accurate than the conventional one in which the difference of pixel information was used. However, when the SWI result has considerable noise or has been distorted from the internal region in brain, the accuracy of detection becomes low. This limitation should be complemented by further research on image improvement. This paper aimed to verify the possibility of improvement in computer processing by adopting the MR theory. Further research needs to be conducted to help in resolving the general limitations through the appropriate combination of MR theory and computer science.

Acknowledgement

This study was supported by a grant of the Korean Health Technology R&D Project, Ministry of Health & Welfare, Republic of Korea (A112020).

References

[1] S. Hemachande, A. Verma, S. Arora and Prasanta K. Panigrahi, “Locally Adaptive Block Thresholding Method with Continuity Constraint”, Pattern Recognition Letters, vol. 28, **(2007)**, pp. 119-124.
[2] C. C. Kang and W. J. Wang, “A Novel Edge Detection Method Based on Maximization of the Objective Function”, Pattern Recognition, vol. 40, no. 2, **(2007)**, pp. 609-618.
[3] R. C. Gonzalez and P. Wintz, “Digital Image Processing”, 3rd Ed., Addison-Wesley, **(1993)**.
[4] N. Baba, N. Ichse and T. Tanaka, “Image Area Extraction of Biological Objects from a Thin Section Image by Statistical Texture Analysis”, Electron Microse, vol. 45, **(1996)**, pp. 298-306.
[5] J. L Muerle and D. C.Allen, “Experimental Evaluation of a Technique for Automatic Segmentation of Objects in Complex Scenes”, IPPR, Thopmson, **(1968)**.
[6] M. Unser, “Texture Classification and Segmentation for Using Wavelet Frames”, IEEE Trans., vol. 4, no. 11, **(1995)**, pp. 1549-1560.
[7] W. Li, C. Zhou and Z. Zhang, “Segmentation of the body of the tongue based on the improved snake algorithm in traditional Chinese medicine”, Proc. of the 5th World Congress on Intelligent Control and Automation, **(2004)**, pp. 15-19.
[8] R. Zabih and V. Kolmogorov, “Spatially coherent clustering using graph cuts”, Proc. of Computer Vision and Pattern Recognition, vol. 2, **(2004)**, pp. 437-444.
[9] C. Rother, V. Kolmogorov and A. Blake, “GrabCut: Interactive foreground extraction using iterated graph cuts”, ACM Trans. Graphics, vol. 23, no. 3, **(2004)**, pp. 309-314.
[10] M. Kass and A. Witkin, “Demetri Terzopoulos Active Contour Models”, International Journal of Computer Vision, vol. 1, **(1988)**, pp. 321-331.
[11] E. Y. K. Ng and Y. Chen, “Segmentation of the Breast Thermogram: Improved Boundary Detection with the Modified Snake Algorithm”, Journal of Mechanics in Medicine and Biology, vol. 6, no. 2, **(2006)**, pp. 123-136.
[12] D. Joong Kang and I. So Kweon, “A fast and stable snake algorithm for medical images”, Pattern Recognition Letters, vol. 20, no. 10, , **(1999)**, pp. 1069.
[13] R. I. Shrager, G. H. Weiss and R. G. S. Spence, NMR Biomed., vol. 11, **(1998)**, pp. 297-305.
[14] R. V. Damadian, Science, vol. 171, **(1971)**, pp. 1151-1153.
[15] R. A. de Graaf, P. B. Brown, S. McIntyre, T. W. Nixon, K. L. Behar and D. L. Rothman, Magn. Reson.Med., vol. 56, **(2006)**, pp. 386-394.

[16] E. M. Haacke, Y. Xu, Y. C. Cheng and J. R. Reichenbach, "Susceptibility weighted imaging (SWI)", Magn Reson Med, vol. 52, **(2004)**, pp. 612-618.
[17] Y. C. Cheng, E. M. Haacke and Y. J. Yu, "An exact form for the magnetic field density of states for a dipole", Magn Reson Imaging, vol. 19, **(2001),** pp. 1017-23.
[18] L. R. Schad, "Improved target volume characterization in stereotactic treatment planning of brain lesions by using high-resolution BOLD MR-venography", NMR Biomed, vol. 14, **(2001)**, pp. 478-83.
[19] J. R. Reichenbach and E. M. Haacke, "High-resolution BOLD venographic imaging; a window into brain function", NMR Biomed, pp. 14, **(2001)**, pp. 453-67.
[20] J. R. Reichenbach, L. Jonetz-Mentzel and C. Fitzek, "High-resolution blood oxygen-level dependent MR venography (HRBV): a new technique", Neuroradiology, vol. 43, **(2001)**, pp. 364-69.
[21] Y. Wang, Y. Yu and D. Li, "Artery and vein separation using susceptibilitydependent phase in contrast-enhanced MRA", J Magn Reson Imaging, vol. 12, **(2000)**, pp. 661-70.
[22] M. A. Fernandez-Seara, A. Techawiboonwong and J. A. Detre, "MR susceptometry for measuring global brain oxygen extraction", Magn Reson Med, vol. 55, **(2006)**, pp. 967-73.
[23] E. M. Haacke, M. Ayaz and A. Khan, "Establishing a baseline phase behavior in magnetic resonance imaging to determine normal vs. abnormal iron content in the brain", Magn Reson Imaging, vol. 26, **(2007)**, pp. 256-64.
[24] S. Ogawa, T. M. Lee, A. R. Kay and D. W. Tank, "Brain magnetic resonance imaging with contrast dependent on blood oxygenation", Proc Natl Acad SciUSA, vol. 87, **(1990)**, pp. 9868-9872.
[25] S. Ogawa and T. M. Lee, "Magnetic resonance imaging of blood vessels at high fields: in vivo and in vitro measurements and image simulation", Magn Reson Med, vol. 16, **(1990)**, pp. 9-18.
[26] S. Ogawa and T. M. Lee, A. S. Nayak and P. Glynn, "Oxygenation-sensitive contrast in magnetic resonance image of rodent brain at high magnetic fields", Magn Reson Med, vol. 14, **(1990)**, pp. 68-78.
[27] R. J. Ogg, J. W. Langston, E. M. Haacke, R. G. Steen and J. S. Taylor, "The correlation between phase shifts in gradient-echo MR images and regional brain iron concentration", Magn Reson Imaging, vol. 17, **(1999)**, pp. 1141-1148.
[28] W. T. Dixon, "Simple proton spectroscopic imaging", Radiology, vol. 153, **(1984)**, pp. 189-194.
[29] E. M. Haacke, J. L. Patrick, G. W. Lenz and T. Parrish, "The separation of water and lipid components in the presence of field inhomogeneities", Rev Magn Reson Med, vol. 1, **(1986)**, pp. 123-154.
[30] J. R. Reichenbach, M. Essig, E. M. Haacke, B. C. Lee, C. Przetak, W. A. Kaiser and L. R. Schad, "High resolution venography of the brain using magnetic resonance imaging", MAGMA, vol. 6, **(1998)**, pp. 62-69.
[31] M. Essig, J. R. Reichenbach, L. R. Schad, S. O. Scho¨nberg, J. Debus and W. A. Kaiser, High-resolution MR venography of cerebral arteriovenous malformations", Magn Reson Imaging, vol. 17, **(1999)**, pp. 1417-1425.
[32] B. C. P. Lee, K. D. Vo, D. K. Kido, P. Mukherjee, J. Reichenbach, W. Lin, M. S. Yoon and E. M. Haacke, "MR high-resolution blood oxygenation level-dependent venography of occult (low-flow) vascular lesions", AJNR Am J Neuroradiol, vol. 20, **(1999)**, pp. 1239-1242.
[33] I. L. Tan, R. A. van Schijndel, P. J. W. Pouwels, M. A. A. van Walderveen, J. R. Reichenbach, R. A. Manoliu and F. Barkhof, "MR venography of multiple sclerosis", AJNR Am J Neuroradiol, vol. 21, **(2000)**, pp. 1039-1042.
[34] K. A. Tong, S. Ashwal, B. A. Holshouser, L. Shutter, G. Herigault, E. M. Haacke and D. K. Kido, "Improved detection of hemorrhagic shearing lesions in children with post-traumatic diffuse axonal injury-initial results", Radiology, vol. 227, **(2003)**, pp. 332-339.
[35] J. R. Reichenbach, L. Jonetz-Mentzel, C. Fitzek, E. M. Haacke, D. K. Kido, B. C. P. Lee and W. A. Kaiser, "High-resolution blood oxygen-level dependent MR venography (HRBV): a new technique", Neuroradiology, vol. 43, **(2001)**, pp.364-369.
[36] K. T. Baudendistel, J. R. Reichenbach, R. Metzner, J. Schroder and L. R. Schad, "Comparison of functional venography and EPI-BOLD-fMRI at 1.5T", Magn Reson Imaging, vol. 16, **(1998)**, pp. 989-991.
[37] J. R. Reichenbach, R. Venkatesan, D. J. Schillinger, D. K. Kido and E. M. Haacke, "Small vessels in the human brain: MR venography with deoxyhemoglobin as an intrinsic contrast agent", Radiology, vol. 204, **(1997)**, pp. 272-277.
[38] D. Comaniciu and P. Meer, "Mean Shift Analysis and Application", Seventh Int'I Conf. Computer Vision and Pattern Recognition, **(1997)**, pp. 750-755.
[39] D. Williams and M. Shah, "A fast algorithm for active contours and curvature estimation", Computer Vision, Graphics, and Image Processing: Image Understanding, vol. 55, **(1992)**, pp. 14-25.

Authors

Eun-Young Jung received Jung received M.S. degree in Health Informatics, Gachon University, Korea, in 2001. She received Ph.D. degree of Medical Informatics from Ajou University, Korea, in 2012. She is currently manager of U-Healthcare Center, Gachon University Gil Medical Center, Korea. Her research interests include u-healthcare, Telecare and Health IT, Virtual Reality simulation.

Sung-Jong Eun received the M.S. degree from Gachon University of South Korea in 2009 and the Ph.D candidate both in Computer Science from Gachon University in 2012. His research areas include Computer Graphics, Medical image processing, Healthcare service, BCI, AR.

Dong Kyun Park received B.S. degree from College of Medicine, Chungbuk National University, Korea, in 1992. He received M.S. and Ph.D. degree in College of Medicine from Inha University, Korea, in 2000 and 2003. He is currently Director of U-Healthcare Center and Medical Specialist of Gastroenterology in Gachon University Gil Medical Center, Korea. His research interests include u-healthcare, RFID, and Big data analysis.